0026-895X/86/040305-10$02.00/0

MOLECULAR PHARMACOLOGY, 30:305-314

Kinetic Studies of [^{3}H]-*N*-Methylscopolamine Binding to Muscarinic Receptors in the Rat Central Nervous System: Evidence for the Existence of Three Classes of Binding Sites

MAGALI WAELBROECK, MICHEL GILLARD, PATRICK ROBBERECHT, and JEAN CHRISTOPHE

Department of Biochemistry and Nutrition, Medical School, Université Libre de Bruxelles, B-1000 Brussels, Belgium (M.W., P.R., J.C.), and Union Chimique Belge, Pharmaceutical Division, Chemin Le Foriest, B-1420 Braine l'Alleud, Belgium (M.G.)

Received November 13, 1985; Accepted July 10, 1986

SUMMARY

We compared the binding of [*N-methyl*-^{3}H]scopolamine methyl chloride ([^{3}H]NMS) and pirenzepine to muscarinic receptors in four regions of the rat central nervous system (cortex, hippocampus, striatum, and cerebellum) and in rat heart. Equilibrium binding studies suggested the existence of three classes of receptors: A, receptors with high affinity for pirenzepine and [^{3}H]NMS (in cortex, hippocampus, and striatum); B, receptors with intermediate affinity for pirenzepine and high affinity for [^{3}H]NMS (in the same brain regions); and C, receptors with low affinity for pirenzepine and [^{3}H]NMS (in cerebellum and heart). Dissociation kinetic studies indicated that the receptor types A, B, and C had different k_{off} values allowing, therefore, a separate study of their binding properties. We observed that : 1) [^{3}H]NMS recognized muscarinic receptors A, B, and C with the following order of potency: B > A ≫ C; and 2) pirenzepine recognized these receptors with a different order of potency: A ≫ B > C. Thus, dissociation kinetics provide a useful tool to identify muscarinic receptor types.

Binding of most antagonists to rat brain muscarinic receptors is consistent with the existence of a single class of noninteracting receptors (1). Little affinity differences are found when comparing homogenates from rat brain and peripheral tissues (see, for example, Ref. 2). These results, together with studies on solubilized receptors (3), suggest that muscarinic receptors are identical in all tissues, the heterogeneity of agonist binding being due to the interaction of receptors with different effector proteins.

Pirenzepine is an unusual atagonist. Indeed, this drug recognizes three receptor classes, depending on the tissue examined. Part of the brain muscarinic receptors has a high affinity for pirenzepine (K_D 20 nM), the remaining sites having a low affinity for this antagonist. The receptors from the lacrimal and parotid glands show an intermediate affinity for pirenzepine (K_D 200 nM). Receptors from heart and smooth muscle have a somewhat lower affinity, with a K_D value of 1000 nM (values taken from Ref. 2).

It has been suggested but not proved that pirenzepine selectivity reflects the interaction of the receptor with effector proteins, rather than receptor heterogeneity per se (4). We shall nevertheless use the term "receptor class" when referring to pirenzepine-defined receptor heterogeneity, since this heterogeneity has been demonstrated in *in vitro* binding experiments as well as in pharmacological studies (5–8).

As suggested above, three classes of pirenzepine-binding sites were initially described. Distinction between the two subclasses with low affinity for pirenzepine was rarely attempted, probably due to the low drug selectivity for these two subclasses. Most studies comparing the pharmacological (9, 10) and biochemical (3, 4, 11, 12) properties of the receptor classes concentrated on differences between "M1" and "M2" receptors with, respectively, high and low affinity for the drug.

We shall demonstrate in this work that: 1) [^{3}H]NMS dissociation kinetics are a very sensitive test for receptor heterogeneity, and 2) three classes of muscarinic receptors are simultaneously present in rat brain. [^{3}H]NMS and pirenzepine recognized these receptors with a rather low selectivity. The presence of this muscarinic receptor heterogeneity has important implications for the interpretation of binding data, the study of solubilized receptors, and pharmacological studies on this tissue.

Experimental Procedures

Materials. [^{3}H]NMS (specific radioactivity 64 Ci/mmol) was obtained from the Radiochemical Center (Amersham, Bucks, England).

This research was aided by Grant 3.4571.85 from the Fonds de la Recherche Scientifique Médicale (Belgium) and a "Concerted action" from the Ministry of Scientific Policy (Belgium).

ABBREVIATIONS: [^{3}H]NMS, [*N-methyl*-^{3}H]scopolamine methyl chloride; I_{50}, concentration of inhibitor causing 50% inhibition of tracer binding; NMS, *N*-methylscopolamine.

[^{3}H]Pirenzepine (specific radioactivity 83 Ci/mmol) was obtained from New England Nuclear (Dreieich, FRG). Pirenzepine (gastrozepin) was kindly provided by Dr. R. Hammer (Institute di Angeli, Milano, Italy). Atropine was from Sigma Chemical Co. (St. Louis, MO).

Methods. Male Wistar albino rats (200–250 g) that had been fed rat chow *ad libitum* were killed by decapitation. The hearts were quickly removed, rinsed at room temperature in isotonic sodium chloride, and then homogenized in 2 ml of ice-cold homogenization buffer (20 mM Tris-HCl buffer, pH 7.5, enriched with 0.25 M sucrose) using an Ultraturrax homogenizer. The homogenate was diluted with the same buffer to 10% (w/v) and filtered through two, then four layers of medical gauze, and stored in liquid nitrogen until use.

The cortex, hippocampus, striatum, and cerebellum were quickly dissected and homogenized in the same buffer (using a glass-Teflon homogenizer). The homogenates [1% (w/v) for [^{3}H]NMS binding studies on cortex, hippocampus and striatum; 10% (w/v) for [^{3}H]NMS binding studies on cerebellum; and 5% (w/v) for all [^{3}H]pirenzepine binding studies] were stored in liquid nitrogen until use.

All protein concentrations were determined using the method of Lowry *et al.* (13) with bovine serum albumin as standard.

Binding assays. Homogenates (400–500 μg of protein for heart and cerebellum; 30–40 μg of protein for cortex, hippocampus, and striatum homogenates) were incubated for 2 hr at 25°, in 1.2 ml of incubation buffer (50 mM sodium phosphate buffer, pH 7.5, enriched with 2 mM $MgCl_2$ and 1% bovine serum albumin), and the indicated concentrations of tracer, and pirenzepine or atropine.

Specific binding was measured as follows. Each sample was filtered on GF/C glass-fiber filters (Whatman, Maidstone, England) and then rinsed four times with 2 ml of ice-cold 50 mM phosphate buffer (pH 7.4). The filters were dried and the radioactivity was counted by liquid scintillation. Nonspecific binding was defined as binding in the presence of 1 μM atropine. This radioactivity was subtracted from total binding, yielding specific binding.

The free tracer concentration was calculated as total minus specific binding (nonspecific binding was due to tracer binding to the GF/C filters).

For Scatchard plot analysis, we maintained the specific binding below 25% of the tracer added. To analyze competition curves with multiple-sites models, we maintained specific binding below 15% of tracer added to limit the alteration in free tracer concentration when unlabeled ligand was added.

Saturation curves. The homogenates were incubated as indicated above, in the presence of [^{3}H]NMS (25–3200 pM) and in the absence or presence of atropine (1 μM). The results were analyzed according to the method of Scatchard (14).

To compare [^{3}H]NMS and [^{3}H]pirenzepine binding, we increased the protein concentration up to 200 μg/assay. The [^{3}H]NMS and [^{3}H]pirenzepine concentration ranges tested were, respectively, 25–3200 pM and 0.4–20 nM. The results were analyzed as above.

Competition curves. The homogenates were incubated as mentioned above, in the presence of a constant [^{3}H]NMS concentration (200 pM unless otherwise indicated) and in the presence or absence of various unlabeled ligand concentrations or of 1 μM atropine. Specific binding was measured as previously indicated. The results were analyzed assuming that the ligand recognized one or two subclasses of muscarinic receptors with different I_{50} values [program developed by Richardson and Humrich (15)].

[^{3}H]NMS dissociation kinetics. The homogenates were preincubated as previously mentioned for 2 hr at 25°. The [^{3}H]NMS concentration was kept at 200 pM unless otherwise indicated.

Following this preincubation, (a) "control" samples were filtered immediately whereas (b) 12-μl aliquots of atropine (1 μM final concentration) were added to all other tubes to induce tracer dissociation. These samples were then filtered at the indicated time intervals after atropine addition.

In some experiments, designed to investigate separately [^{3}H]NMS dissociation from M1 and M2 receptors, we prepared up to seven [^{3}H]NMS-pirenzepine competition curves, as described above. Following the preincubation, a "control competition curve" was filtered immediately. One μM atropine was added to all other samples (see above). Samples for complete competition curves were filtered at the indicated time intervals after atropine addition. The results were analyzed using the computer curve-fitting program (15).

Scatchard plots and competition curve simulation. The [^{3}H]NMS Scatchard plots expected, assuming one, two, or three classes of receptors, were calculated using the following equation:

$$B = \frac{R_1F}{K_1 + F} + \frac{R_2F}{K_2 + F} + \frac{R_3F}{K_3 + F}$$

where R_1, R_2, and R_3 are the three receptor concentrations, K_1, K_2, and K_3 are their respective dissociation constants, and F is the free tracer concentration. The results were plotted according to the method of Scatchard (14).

The [^{3}H]NMS-pirenzepine competition curves expected, assuming one, two, or three classes of receptors, were calculated as follows. (a) [^{3}H]NMS binding to each receptor class was calculated as:

$$B_i = \frac{R_iF}{K_i + F}$$

with i = 1–3. (b) The pirenzepine I_{50} values were calculated according to the method of Cheng and Prusoff (16) for each receptor class:

$$I_i = K_{Pz,i}\left(1 + \frac{F}{K_i}\right)$$

with i = 1–3, where I_i is the pirenzepine I_{50} value for binding to class i receptors and $K_{Pz,i}$ is the pirenzepine K_D value for that receptor class. (c) The [^{3}H]NMS-pirenzepine competition curves were then calculated as:

$$B = \frac{B_1I_1}{I_1 + Pz} + \frac{B_2I_2}{I_2 + Pz} + \frac{B_3I_3}{I_3 + Pz}$$

where Pz is the pirenzepine concentration.

All curves in Figs. 1, 3, 4, 6, and 8–10 were drawn according to the above equations.

Results

Equilibrium [^{3}H]NMS binding. As with most of the so-called nonselective muscarinic antagonists (see, for example, Ref. 2), [^{3}H]NMS recognized the receptors from rat cortex, hippocampus, and striatum with a greater affinity (K_D = 120 ± 20 pM) than the receptors of cerebellum (K_D = 450 ± 60 pM) and heart (K_D = 500 ± 60 pM) (Fig. 1, *top*). The difference between [^{3}H]NMS affinity for cortex, striatum, and hippocampus, on the one hand, and for cerebellum and heart, on the other hand, was significant at the low 25° temperature chosen in our binding studies. [^{3}H]NMS Scatchard plots were linear or almost linear in all preparations tested (see Fig. 1). On the basis of competition curves (Fig. 1, *bottom*), pirenzepine recognized, respectively, 55 ± 10%, 30 ± 8%, and 15 ± 5% of the hippocampus, cortex, and striatum receptors with a high affinity (apparent K_D = 5 ± 2 nM). The remaining receptors showed a low affinity for this selective antagonist (apparent K_D = 120 ± 50 nM) (Fig. 1). The cerebellum and heart receptors had a very low affinity for pirenzepine (K_D = 350 ± 50 nM) (Fig. 1).

Altogether, these results with various rat tissues suggested the existence of three classes or states of muscarinic receptors: A, M1 receptors (with high affinity for pirenzepine), having a high affinity for [^{3}H]NMS (here called the A receptors); B, M2 receptors (with low affinity for pirenzepine), having a high affinity for [^{3}H]NMS (here called the B receptors); and C, M2

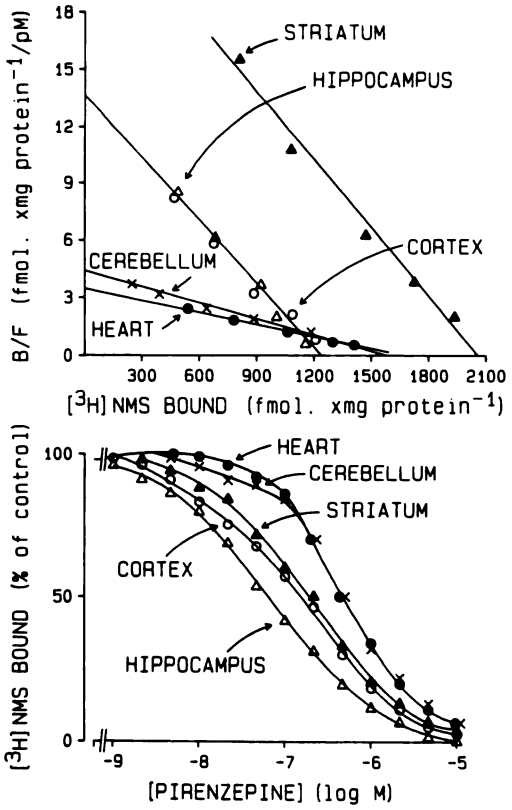

Fig. 1. *Top:* [^{3}H]NMS (150–1600 pM for brain regions and 300–3200 pM for heart) was incubated with striatum (▲), cortex (○), hippocampus (△), cerebellum (×), or heart (●) homogenates. The results are represented according to the method of Scatchard (14). [^{3}H]NMS binding (*B*) was expressed as fmol/mg of protein, except for heart (*B* = fmol/2 mg of protein) and cerebellum (*B* = fmol/10 mg of protein), so that the results could be represented on a comparable scale. The results are representative of at least three experiments performed in duplicate. *Bottom:* [^{3}H]NMS binding to brain or heart homogenates was measured at a constant [^{3}H]NMS concentration (300 pM) and in the absence or presence of the indicated pirenzepine concentrations (*symbols* as in *top*). The results are representative of at least four experiments performed in duplicate.

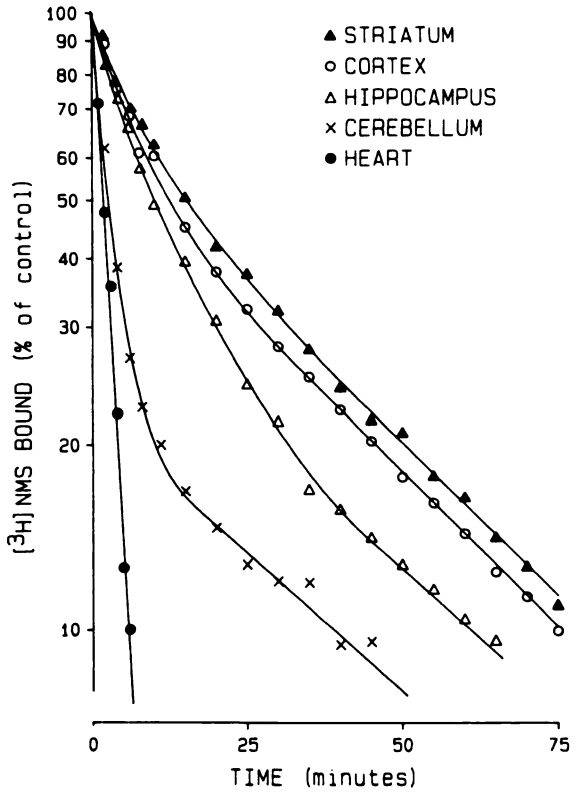

Fig. 2. Striatum (▲), cortex (○), hippocampus (△), cerebellum (×), or heart (●) homogenates were preincubated with 300 pM [^{3}H]NMS for 2 hr at 25°. Atropine (1 μM final concentration) was then added to each sample, and [^{3}H]NMS binding was measured at the indicated time intervals after atropine addition. The results are expressed as percentage of [^{3}H]NMS binding before atropine addition (percentage of control) and are the average of three to four experiments performed in duplicate.

receptors (with low affinity for pirenzepine), having a low affinity for [^{3}H]NMS (here called the C receptors).

The "A" and "B" receptors were observed in cortex, hippocampus, and striatum, the "C" receptors being found in the cerebellum and heart (Fig. 1).

The binding properties of [^{3}H]NMS and pirenzepine to these three receptor classes and their exact localization shall be discussed below, once dissociation kinetics have been analyzed.

Dissociation kinetics: evidence for [^{3}H]NMS selectivity. When studying [^{3}H]NMS dissociation kinetics, we observed rapid, first order dissociation from rat heart homogenate receptors with a k_{off} value of 0.35 ± 0.06 min^{-1} (Fig. 2). By contrast, [^{3}H]NMS dissociation from the three brain regions studied and from the cerebellum was biphasic (Fig. 2).

We were struck by the correlation between the proportion of sites with low affinity for pirenzepine (70, 85, and 45%) and the proportion of slowly dissociating NMS sites (60, 70, and 40%) in, respectively, the cortex, striatum, and hippocampus (compare Figs. 1 and 2). This correlation suggested that three muscarinic receptor classes with different [^{3}H]NMS dissociation rate constants were present: A receptors having an intermediate dissociation rate constant, B receptors with a very low dissociation rate constant, and C receptors having a very large dissociation rate constant (see Fig. 2). (The k_{off} values of these three sites will be given below.)

Pilot experiments, using cortex homogenates, indicated that pirenzepine inhibited [^{3}H]NMS binding to the rapidly dissociating receptors with a greater affinity than [^{3}H]NMS binding to the slowly dissociating receptors. These results supported the hypothesis that A and B receptor classes had different [^{3}H]NMS dissociation rate constants.

The following experiments were designed to measure the [^{3}H]NMS dissociation rate constant from A and B receptors and to measure their affinities for the tracer. We first checked that slowly dissociating receptors had a low affinity for pirenzepine. To achieve this aim, we: 1) performed competition curves using [^{3}H]NMS as tracer and pirenzepine or atropine as unlabeled competitor, 2) induced tracer dissociation by atropine addition, and 3) measured [^{3}H]NMS binding following a 35-min dissociation period.

As shown in Fig. 3 (*left*), [^{3}H]NMS-atropine competition curves had a Hill coefficient of 1.0 ± 0.03, indicating that atropine recognized all brain muscarinic receptors with the same high affinity (I_{50} = 0.6 ± 0.2 nM). After 35 min of dissociation, [^{3}H]NMS bound mainly to slowly dissociating receptors (see Fig. 2). Atropine inhibited [^{3}H]NMS binding to the slowly dissociating receptors with the same potency as [^{3}H]NMS binding to total receptors (control), confirming that it behaved as a nonselective antagonist.

As shown in Fig. 3 (*right*), pirenzepine inhibited [^{3}H]NMS binding to slowly dissociating receptors with a very low potency

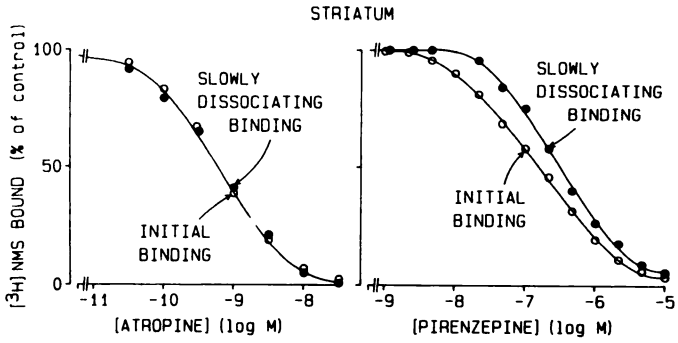

Fig. 3. [^{3}H]NMS (250 pM) was preincubated with striatum homogenate for 2 hr at 25° in the absence or presence of the indicated atropine (*left*) or pirenzepine (*right*) concentrations. Following this preincubation: (1) duplicate samples were filtered to measure the initial binding (○) or (2) 1 μM atropine was added to other duplicate samples, to induce isotopic dilution. These samples were filtered 35 min after atropine addition (slowly dissociating, ●). All results were expressed as percentage of [^{3}H] NMS binding in the absence of competitor. These results are representative of three experiments performed on hippocampus, cortex, and striatum.

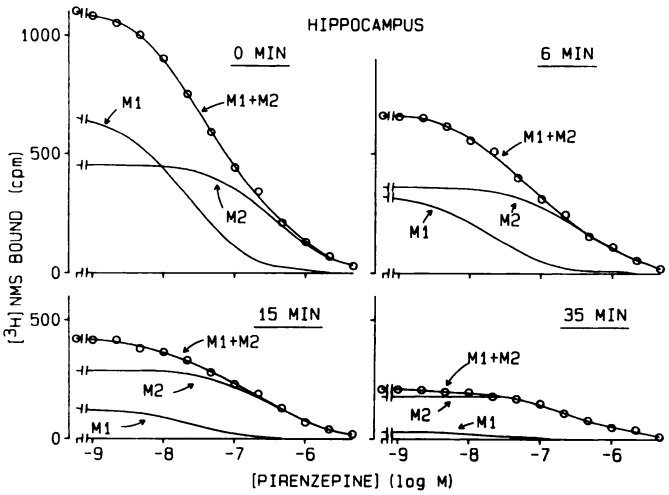

Fig. 4. Hippocampus homogenates were preincubated for 2 hr at 25° in the presence of 250 pM [^{3}H]NMS and in the absence or presence of the indicated pirenzepine concentrations. Duplicate samples were filtered immediately (initial, *top left*). Atropine (1 μM final concentration) was added to the other samples to induce isotopic dilution, and duplicate samples were filtered 6 min (*top right*), 15 min (*bottom left*), or 35 min (*bottom right*) after atropine addition. ○, experimentally measured [^{3}H] NMS specific binding (expressed in cpm). Nonspecific binding was 50 cpm. The *lines* represent [^{3}H]NMS binding to M1, M2, and M1 + M2 receptors found by computer curve fitting of the competition curves (15). This experiment is representative of three experiments on hippocampus and two experiments on cortex and striatum.

(Hill coefficients, 0.93 ± 0.05; I_{50} 380 ± 40 nM). This contrasted with pirenzepine inhibition of [^{3}H]NMS binding to total receptors (Hill coefficient 0.8 ± 0.05; I_{50} 160 ± 30 nM). Analysis of these competition curves, assuming the existence of two receptor classes, indicated that the proportion of A (M1) receptors labeled by [^{3}H]NMS decreased from 55 ± 10% to 10 ± 5% in hippocampus, from 30 ± 8% to 3 ± 2% in cortex, and from 15 ± 5% to nondetectable values in striatum, when the tracer was allowed to dissociate from most of its rapidly dissociating receptors. These results confirmed that the slowly dissociating muscarinic receptors labeled by [^{3}H]NMS in rat brain had a low affinity for pirenzepine.

To measure the [^{3}H]NMS dissociation rate from M1 (A) and M2 (B) receptors, we performed the same experiment as above, but allowed [^{3}H]NMS to dissociate for various short time intervals. As shown in Fig. 4, the pirenzepine potency decreased progressively with [^{3}H]NMS dissociation. The competition curves were analyzed assuming the presence of two classes of binding sites (15). The pirenzepine I_{50} values for M1 and M2 receptors (I_1 and I_2) did not change significantly during this experiment. By contrast, tracer binding to M1 (A) receptors decreased faster (50% decrease after 6 min of dissociation) than tracer binding to M2 receptors (50% decrease after more than 15 min of dissociation) (Fig. 4).

[^{3}H]NMS dissociation from M1 receptors was monophasic, with a k_{off} value of 0.10 min^{-1} (Fig. 5). The initial [^{3}H]NMS binding to M2 receptors was greater than expected from a monophasic dissociation rate. The discrepancy was small. It was, however, our first indication that brain M2 receptors might be heterogeneous (Fig. 5). A majority (80%) of the receptors had a very low dissociation rate (k_{off} 0.02 min^{-1}). We did not attempt to calculate the rapid [^{3}H]NMS dissociation rate from the remaining 20% of M2 receptors.

[^{3}H]NMS Scatchard plots and [^{3}H]NMS-pirenzepine competition curves were compatible with the assumption that [^{3}H] NMS recognized two classes of "pirenzepine receptors" (with pirenzepine K_i values of 4 and 125 nM) with the same high affinity (K_D 150 pM) (Fig. 6).

Using Scatchard plots, we were not able to detect lower tracer selectivity (below 4- to 5-fold). Theoretically, however, variations of the proportions of rapidly and slowly dissociating receptors with changes in tracer concentration can be readily demonstrated when the tracer selectivity is correlated with different dissociation rate constants. This is because the receptors with highest affinity for the tracer are saturated at lower concentrations than are the remaining receptors. We therefore measured the [^{3}H]NMS dissociation rate from receptors preincubated with various tracer concentrations.

As shown in Fig. 7 (*top*), the [^{3}H]NMS dissociation rate was markedly occupancy dependent. At low tracer concentration (50 pM), when only 15% of the receptors were occupied, 30% of the bound tracer dissociated rapidly (k_{off} = 0.12 min^{-1}) and the remaining 70% dissociated slowly (k_{off} = 0.02 min^{-1}). At the highest tracer concentration investigated, when 93% of the receptors were occupied, 44% of the bound tracer dissociated slowly (k_{off} = 0.02 min^{-1}). The remaining 56% dissociated very rapidly. The dissociation kinetics of rapidly dissociating receptors were slightly biphasic, suggesting that these receptors might be heterogeneous. We calculated [^{3}H]NMS binding to the rapidly and slowly dissociating receptors at various [^{3}H] NMS concentrations (as shown in Fig. 7, *top*, for two tracer concentrations) and then plotted these results according to the method of Scatchard (14) (Fig. 7, *bottom*). The data confirmed that the slowly dissociating receptors had a greater affinity for [^{3}H]NMS (K_D = 90 pM) than did the rapidly dissociating receptors (K_D = 360 pM).

As shown in Fig. 8 (*bottom*), our equilibrium binding data were not compatible with the hypothesis that [^{3}H]NMS had a high affinity (K_D = 90 pM) for M2 (B) receptors and a low affinity (K_D = 360 pM) for M1 (A) receptors. In Fig. 8 (*top*), the [^{3}H]NMS Scatchard plot expected, assuming a 4-fold selectivity, was almost linear and compatible with our experimental data.

By contrast, we would expect, within a two-site model, that

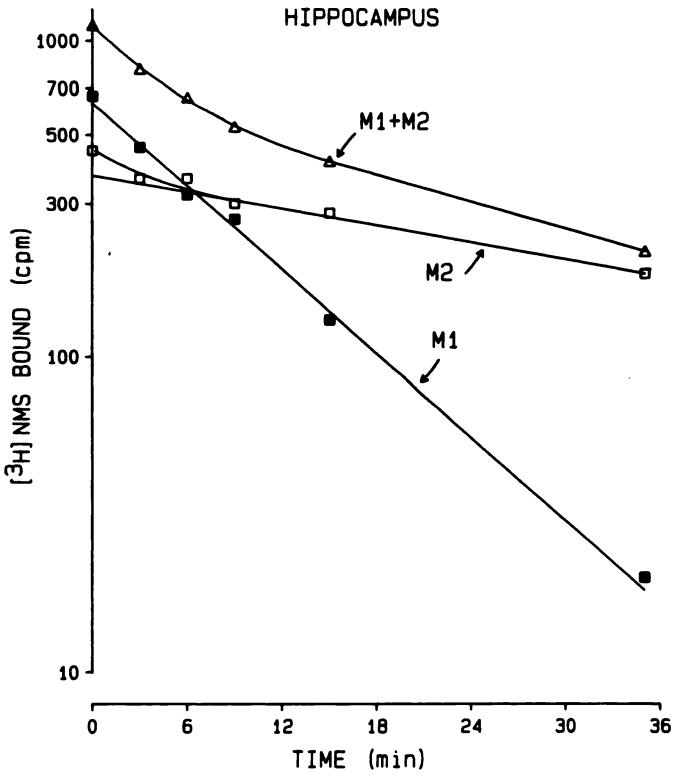

Fig. 5. [^{3}H]NMS-pirenzepine competition curves obtained at various times after atropine addition (some of which are shown in Fig. 4) were analyzed to measure the contribution of M1 and M2 receptors to total [^{3}H]NMS binding. Total [^{3}H]NMS binding (△) was compared with [^{3}H] NMS binding to M1 receptors (■) and [^{3}H]NMS binding to M2 receptors (□), as a function of time after atropine addition. The results are expressed as specific [^{3}H]NMS binding, in cpm, on a log scale. This experiment is representative of three experiments on hippocampus and two experiments on cortex and striatum.

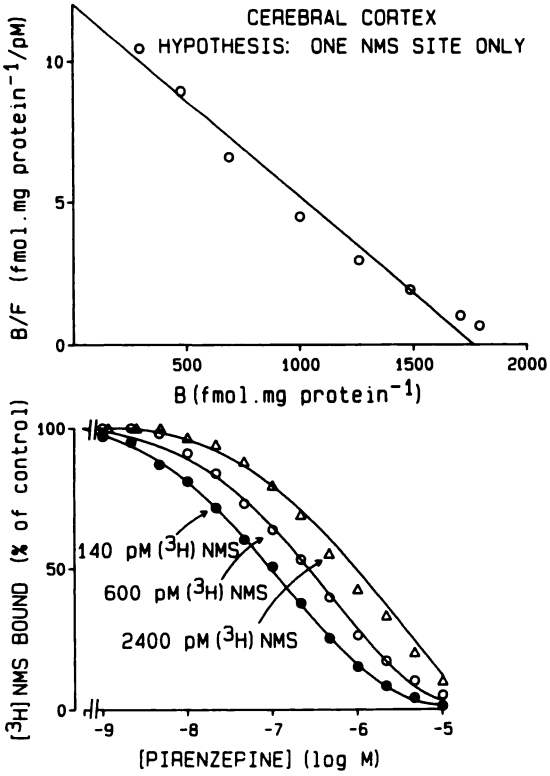

Fig. 6. In this figure, the *symbols* represent experimental data and the *lines* represent fitted curves, using the parameters outlined below. *Top:* A representative [^{3}H]NMS Scatchard plot obtained with cortex homogenates (○) was fitted assuming a single class of receptors (1800 fmol/mg of protein, K_D 150 pM) (one experiment representative of 10 experiments performed in duplicate). *Bottom:* [^{3}H]NMS ●, 140 pM; ○, 600 pM; or △, 2400 pM) was incubated in the absence or presence of the indicated pirenzepine concentration with cortex homogenates. The results are compared to the curves expected if 30% of the receptors had K_D values of 125 pM [^{3}H]NMS and 4.0 nM for pirenzepine, the remaining 70% having a K_D value of 125 pM for [^{3}H]NMS and 130 nM for pirenzepine [best fit parameters for the competition curve obtained at 120 pM [^{3}H] NMS (15)].

the proportion of [^{3}H]NMS bound to M1 receptors would increase with increasing tracer concentration (in parallel with the increase of rapidly dissociating tracer shown in Fig. 5). We also would expect that the pirenzepine I_{50} value for M1 sites (I_1) would be less "tracer dependent" than the pirenzepine I_{50} value for M2 sites (I_2) due to the lower [^{3}H]NMS affinity for M1 receptors (the expected competition curves, calculated as explained in Experimental Procedures, are shown in Fig. 8).

These two effects of tracer concentration on pirenzepine competition curves were totally absent. This was not entirely surprising, as we had previously noted that: 1) part of the M2 receptors had a very large [^{3}H]NMS dissociation rate (Fig. 5), and 2) the rapidly dissociating receptors were heterogeneous, a receptor class dissociating [^{3}H]NMS very rapidly being labeled only at very large tracer concentrations (Fig. 7, *top*).

More than 90% of the receptors found in cerebellum had [^{3}H]NMS- and pirenzepine-binding properties very similar to those of cardiac muscarinic receptors, i.e., low affinity for pirenzepine, low affinity for [^{3}H]NMS, and a large [^{3}H]NMS dissociation rate constant (Figs. 1 and 2). We therefore wondered whether C receptors might be present in the cortex, hippocampus, and striatum.

Inclusion of a third receptor class with "cardiac binding properties" ([^{3}H]NMS K_D, 500 pM; pirenzepine K_D value, 350 nM) allowed us to fit the equilibrium binding data, as shown in Fig. 7. We estimated that the proportions of A, B, and C receptors were approximately equal in cortex homogenates (using dissociation kinetics analysis; Fig. 5). As a first approximation, we assumed that the three [^{3}H]NMS K_D values were proportional to the three dissociation rate constants (that is, that the three [^{3}H]NMS association rate constants were identical). Using these parameters, we calculated the "expected" Scatchard plot and competition curves, as above. A very reasonable fit of the binding data could be obtained using these parameters (not shown). The "expected" average [^{3}H]NMS K_D values (90 pM) were, however, definitely lower than the generally observed K_D values (average, 120 pM). A higher K_D value for [^{3}H]NMS binding to B sites (Fig. 7) was necessary to fit the Scatchard plots and competition curves (Fig. 9). The above fitting of curves indicated that the presence of "B" receptors (with very high affinity for [^{3}H]NMS) was masked in competition curves by "C" receptors (with very low affinity for [^{3}H] NMS). The proportion of M1 receptors did not vary significantly with tracer concentration. Indeed, the decreased proportion of slowly dissociating M2 receptors (B receptors) at high tracer concentrations (Fig. 5) was compensated by an increase of the proportion of rapidly dissociating M2 receptors (C receptors).

The [^{3}H]NMS K_D values could not be calculated by this curve-fitting procedure. Indeed, nine parameters were needed

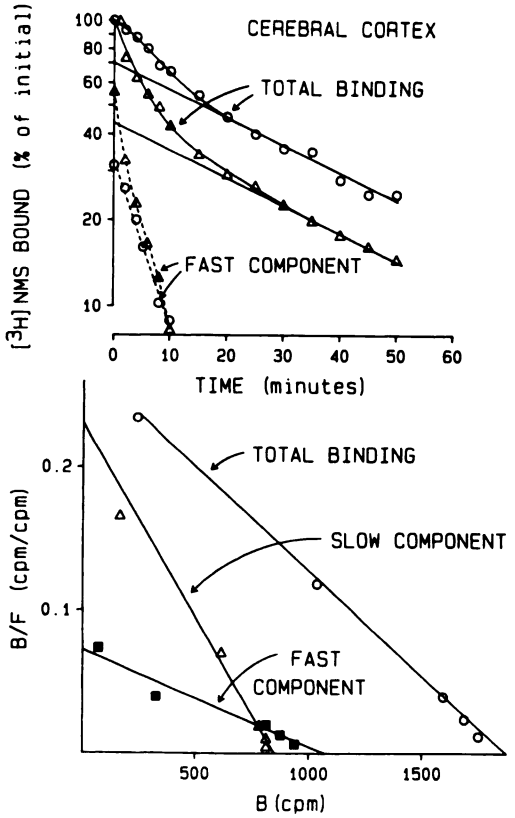

Fig. 7. *Top:* Cortex homogenates were preincubated for 2 hr at 25° in the presence of 60 pM (○) or 4000 pM (△) [^{3}H]NMS. Atropine (1 μM) was then added to each tube and specific binding was measured at the indicated time intervals following isotopic dilution (*TOTAL BINDING*). [^{3}H] NMS dissociation from the rapidly dissociating receptors was then calculated after subtraction of the slow component (– – –, *FAST COMPONENT*). *Bottom:* [^{3}H]NMS dissociation curves were obtained after preincubation with various [^{3}H]NMS concentrations (60–4000 pM) as above. Two of these dissociation curves are shown. *TOTAL BINDING* (○) represents [^{3}H]NMS binding before atropine addition, according to the method of Scatchard (14). The contribution of the "slow" and "fast" (total minus slow) components to total [^{3}H]NMS binding was measured by dissociation kinetic analysis (as shown in the *top panel* for two tracer concentrations). These results were also represented according to the method of Scatchard (14), calculating the free tracer concentration as tracer added minus total binding. These results are representative of at least three experiments performed on cortex and two experiments performed on both hippocampus and striatum.

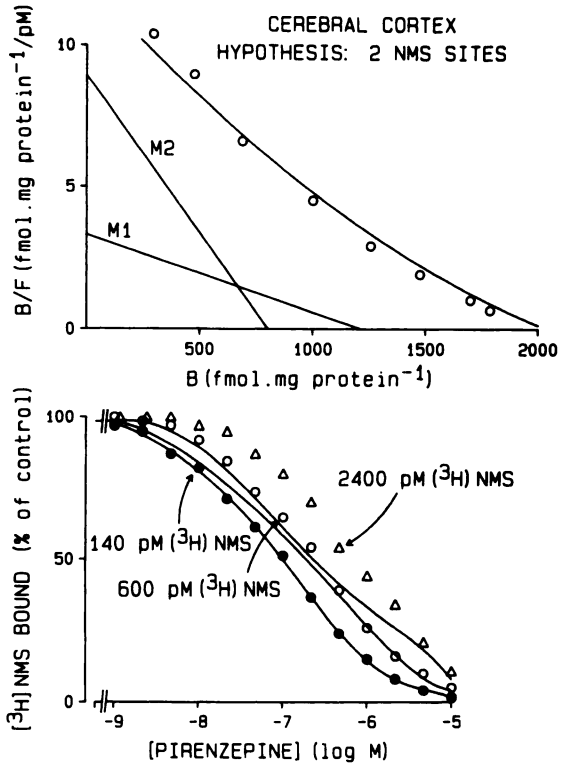

Fig. 8. The experimental results shown are identical to the results shown in Fig. 6. The *lines* represent [^{3}H]NMS Scatchard plot and competition curves expected if 60% of the receptors had K_D values of 360 pM for [^{3}H]NMS and 9.1 nM for pirenzepine and 40% of the receptors had K_D values of 90 pM for [^{3}H]NMS and 130 nM for pirenzepine (B_{max} and [^{3}H] NMS K_D values were taken from Fig. 7; the pirenzepine K_D value corresponded to the best fit of the competition curve obtained with 140 pM [^{3}H]NMS).

to build the competition curves shown in Fig. 7 (three receptor concentrations, three [^{3}H]NMS K_D values, and three pirenzepine K_D values). The results shown in Figs. 3, 7, 8, and 9 simply indicated that three classes of receptors were necessary to fit all experimental data.

Estimate of the [^{3}H]NMS selectivity for A and B receptors. [^{3}H]NMS selectivity should be readily detectable, provided that binding to "C" receptors is prevented. To achieve this aim, we simply allowed the tracer to dissociate for 15 min. Under these conditions, the tracer bound to C receptors was totally dissociated, whereas tracer binding to A and B receptors was still readily demonstrated, either by competition curves or by dissociation kinetics analysis (see Fig. 2).

We compared the [^{3}H]NMS-pirenzepine competition curves obtained under these conditions, at two tracer concentrations (200 and 2000 pM). The competition curves were almost parallel (not shown), but tracer selectivity was detectable in three of four experiments. Indeed, the M1 receptor proportion labeled by [^{3}H]NMS was 20–30% higher and the pirenzepine selectivity 1.5- to 2.0-fold greater at the larger 2000 pM [^{3}H]NMS concentration used. These results indicated that [^{3}H]NMS recognized B receptors with an affinity 2- to 3-fold greater than that of A receptors.

Our best estimates for [^{3}H]NMS and pirenzepine K_D values (using all of the above experimental data) are shown in Table 1. The proportions of A, B, and C receptors found in the various brain regions and cerebellum are shown (approximate values) in Table 2.

High [^{3}H]pirenzepine binding. M1 receptor proportions as high as 80% for hippocampus muscarinic receptors (17) or 65% for cortex muscarinic receptors (18) have been described previously. We obtained similar results when measuring [^{3}H] NMS and [^{3}H]pirenzepine (0.8–13.0 nM) binding under the same experimental conditions. Indeed, [^{3}H]pirenzepine labeled, respectively, 85 ± 10%, 50 ± 14%, and 30 ± 8% of the [^{3}H] NMS-labeled receptors in hippocampus, cortex and striatum homogenates (not shown). The [^{3}H]pirenzepine K_D value was 10 ± 3 nM in the three brain regions studied. We were unable to use these K_D values or M1 receptor proportions to fit the [^{3}H]pirenzepine-pirenzepine and [^{3}H]NMS-pirenzepine competition curves at various tracer concentrations (2–13 nM [^{3}H] pirenzepine, 40–3000 pM [^{3}H]NMS). All of these competition curves were singificantly better fitted when assuming that the [^{3}H]pirenzepine-labeled receptors and 20, 30, or 50% of the [^{3}H]NMS-labeled receptors (in striatum, cortex, and hippocampus) had an unlabeled pirenzepine K_D value of 4–6 nM. We

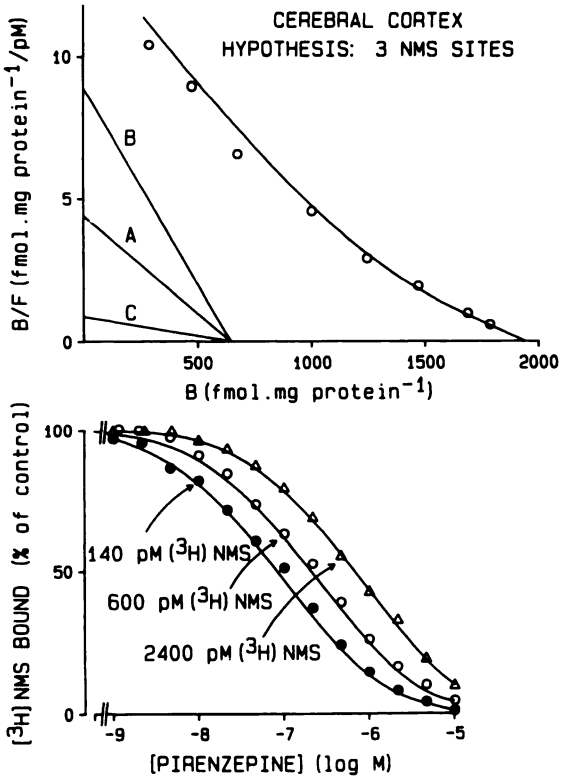

Fig. 9. The experimental results shown are identical to those in Fig. 6. The *lines* represent the [^{3}H]NMS Scatchard plot and competition curves expected if one-third of the receptors had a K_D value of 150 pM for [^{3}H] NMS and 8 nM for pirenzepine, one third of the receptors had a K_D value of 75 pM for [^{3}H]NMS and 50 nM for pirenzepine, and one-third of the receptors had a K_D value of 500 pM for [^{3}H]NMS and 350 nM for pirenzepine.

TABLE 1

Best estimates for [^{3}H]NMS and pirenzepine K_D values

Receptor type	[^{3}H]NMD K_D	Pirenzepine K_D
	pM	*nM*
Brain A	150–200	6–8
Brain B	50–100	50–90
Heart (similar to C receptors)	500 ± 60	350 ± 50

TABLE 2

Proportions of A, B, and C receptors found in various brain regions and cerebellum

	A	B	C
		%	
Cortex	25–35	25–35	25–35
Hippocampus	50–60	20–30	10–20
Striatum	15–25	40–60	30–40
Cerebellum	ND[a]	10–15	80–90

[a] ND, not detectable (i.e., <10%).

therefore wondered whether [^{3}H]pirenzepine binding to B receptors, undetected in the small tracer concentration range we usually used, might be responsible for overestimations of the M1 receptor proportion and K_D values when using Scatchard plot analysis of [^{3}H]pirenzepine saturation curves. Theoretical results, shown in Fig. 10, suggested that: 1) [^{3}H]pirenzepine concentrations well above 50 nM are necessary to detect receptor heterogeneity, 2) binding to the B receptors profoundly alters the Scatchard plot in the low [^{3}H]pirenzepine concentration range, and 3) if [^{3}H]pirenzepine dissociates from C but not B receptors, deviations from a linear Scatchard plot are small and are detectable only if an unusually large concentration range (above 100-fold) is used.

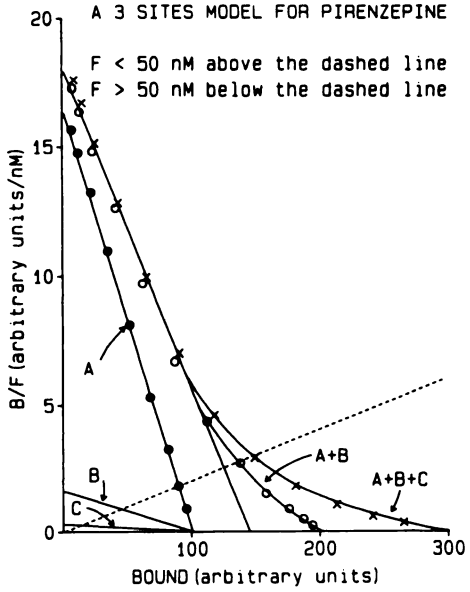

Fig. 10. All data in this figure are theoretical. It shows the Scatchard plots expected if a labeled ligand (for example, [^{3}H]pirenzepine) recognized one, two, or three classes of receptors, with K_D values of 6 nM (●), 6 and 60 nM (○), or 6, 60, and 350 nM (×). The concentrations of each site were taken as 100 (arbitrary units). The data expected at free tracer concentrations below 50 nM are found *above* the *dashed line*. The data expected at free tracer concentrations above 50 nM are found *below* the *dashed line*. When assuming the existence of two or three sites, the deviation from a linear Scatchard plot was below 10% of the bound tracer, at free tracer concentrations below 50 nM.

To test the hypothesis that [^{3}H]pirenzepine may label B and/or C receptors under filtration conditions, we decided to measure a saturation curve using tracer concentrations from 0.6 to 350 nM. To obtain a good specific/nonspecific binding ratio, we modified the usual protocol as explained in the legend of Fig. 11 and carefully verified that these modifications did not modify the [^{3}H]NMS and [^{3}H]pirenzepine binding properties described above. As shown on Fig. 11, [^{3}H]pirenzepine data deviated slightly, but systematically, from results expected assuming a single receptor subclass labeled by this tracer. The saturation curve gave a significantly better fit (15) when assuming that almost equal concentrations of two receptors (K_D = 6 and 80 nM) were responsible for [^{3}H]pirenzepine binding. This result suggested that [^{3}H]pirenzepine dissociates from C but not from B receptors during the filtration procedure.

Discussion

As discussed in the introduction, the initial report of pirenzepine selectivity suggested the existence of three, rather than two, classes of muscarinic receptors (2). The receptors with highest affinity for pirenzepine were found in neuronal tissues (brain and human stellate ganglion). The receptors from secretory glands had an intermediate affinity for pirenzepine, those from heart and smooth muscle having the lowest affinity for this selective antagonist (2).

By contrast, with rat heart muscarinic receptors, dissociation of labeled muscarinic antagonists from most brain regions is

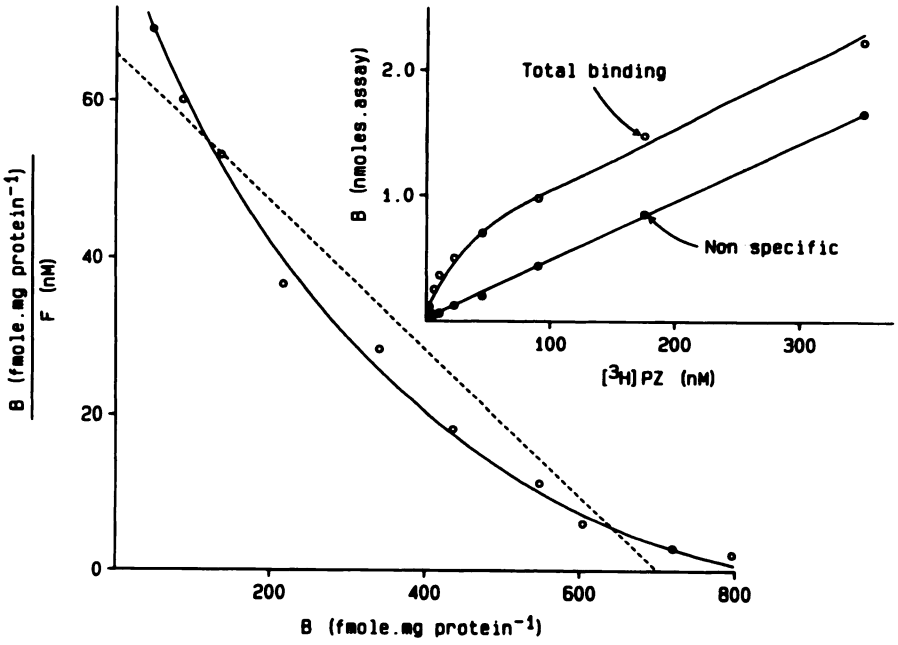

Fig. 11. A [^{3}H]pirenzepine ([^{3}H]PZ) saturation curve obtained in cortex homogenate, using tracer concentrations from 0.6 to 350 nM. To achieve this experiment we: 1) diluted [^{3}H]pirenzepine 5-fold with unlabeled pirenzepine to increase the tracer concentration, 2) decreased the assay volume to 600 μl, 3) increased the protein concentration to 0.9 mg of protein/assay, and 4) presoaked the GF/C filters overnight in 0.05% polyethyleneimine (Sigma Chemical Co.) in order to reduce nonspecific binding. (We previously checked that these technical modifications were unable, per se to affect any of the results presented in this paper.) [^{3}H]Pirenzepine binding data (shown in the *inset*) were transformed according to the method of Scatchard (14). – – –, linear regression of the Scatchard plot (K_D = 10.6 nM, receptor concentration, 700 fmol/mg of protein). The *curve* represents the fit obtained when assuming two receptor classes: 428 fmol/mg of protein (K_D = 6 nM) and 440 fmol/mg of protein (K_D = 80 nM). The two-site fit was found to be significantly better than the best one-site fit, using the program described in Ref. 15.

"biphasic" (see Refs. 19–22). This result is generally interpreted as evidence for ligand-induced receptor isomerization to a slowly dissociating state. According to this model ($L + R = LR = LR'$), the proportion of isomerized receptors (LR') varies from tissue to tissue, reflecting changes in the isomerization constant. The proportion of isomerized receptors within a tissue is, however, *independent* of the receptor occupancy. Kloog and Sokolovsky (19) found no effect of the degree of receptor occupancy by the tracer [^{3}H]atropine on the dissociation rate, a result compatible with antagonist-induced receptor isomerization rather than with receptor heterogeneity. However, as pointed out by Laduron *et al.* (20), the results of association and dissociation kinetics studies, assuming one isomerizable receptor versus two receptors with the same affinity for the tracer, are very similar.

Most classical muscarinic antagonists recognize the receptors from forebrain with a higher affinity than the receptors from cerebellum (21, 22), heart (23), and ileum (24). This selectivity is, however, low and therefore difficult to use for receptor classification. Until recently, pirenzepine was the only known antagonist capable of detecting receptor heterogeneity within a tissue in equilibrium studies [with the exception of [^{3}H] quinuclidinylbenzilate binding to cat brain synaptic membranes (25)]. Recent results suggest that dicyclomine (26) recognizes a minor population of low affinity sites in cortex.

Dissociation kinetics are useful to demonstrate the existence of different receptor types, even when the tracer selectivity is very low. This type of study allowed Tolkovsky (27) to demonstrate the existence of two opiate receptors with the same affinity for the tracer but different kinetic constants and Trifiletti *et al.* (28) to show kinetic differences between two types of benzodiazepine receptors.

We used a similar approach to demonstrate that: (a) [^{3}H] NMS recognized three classes of muscarinic receptors with different kinetic constants and equilibrium dissociation constants, in rat brain; (b) pirenzepine recognized the same three receptor subclasses, with a different order of potency; and (c) the three receptor classes were represented in cortex, hippocampus, and striatum, whereas two receptor classes only (with low affinity for pirenzepine) were present in cerebellum.

We were led to this conclusion by three observations. (a) At equilibrium, the muscarinic receptors from cerebellum did not behave in a manner comparable to that of receptors from cortex, striatum, and hippocampus. The cerebellum receptors presented a lower affinity for [^{3}H]NMS (K_D 450 pM) and for pirenzepine (K_D 350 nM) than did M2 receptors from cortex, hippocampus, and striatum (K_D values of 120 pM and 120 nM for [^{3}H]NMS and pirenzepine, respectively).

(b) Dissociation kinetics, using a low tracer concentration, suggested the existence of three receptor classes with different k_{off} values: 80% of the [^{3}H]NMS bound to cerebellum receptors dissociated with a very large k_{off} value (0.35 min^{-1}); more than 80% of the [^{3}H]NMS bound to M2 receptors from cortex, hippocampus, and striatum dissociated with a very low k_{off} value (0.02 min^{-1}); and the [^{3}H]NMS bound to M1 receptors dissociated with an intermediate k_{off} value (0.10 min^{-1}).

(c) Comparison of dissociation kinetics obtained after preincubation with low and high tracer concentrations (ranging from 60 to 2000 pM) indicated the presence of muscarinic receptors with low affinity for [^{3}H]NMS and a very large dissociation rate constant as well as receptors with high affinity for [^{3}H] NMS and a very low dissociation rate constant in cortex, striatum, and hippocampus homogenates. As explained above, this observation could not be explained by receptor isomerization alone and indicated the presence of at least two [^{3}H]NMS-binding sites. Equilibrium binding studies were not compatible with the existence of two [^{3}H]NMS-binding sites with a reverse selectivity for pirenzepine. Introduction of a third binding site with low affinity for [^{3}H]NMS and for pirenzepine was indispensable to fit *both* the kinetic *and* equilibrium data.

Isomerization of the ligand-receptor complex is the best explanation for the observation that allosteric ligands interact cooperatively with muscarinic ligands (Refs. 29–31 and references therein). Ligand-receptor complex isomerization was, however, not sufficient to explain our kinetic data.

NMS is a charged molecule and, therefore, particularly sus-

ceptible to diffusion barriers. It might be argued that the "C" receptors are in fact poorly accessible A or B receptors. The carbamylcholine binding properties appear, however, to contradict this hypothesis: this charged molecule presents a greater average affinity for C receptors, followed by B and A receptors[1] (see Refs. 17 and 18).

Taken together, these data suggest that the three "receptors" detected in this study are different receptors, by contrast with isomerizable states or sites inside and outside hydrophobic vesicles.

It might be argued that the absence of more precise K_D values in the present work is a major failure of our kinetic approach. We feel, however, that the demonstration that [^{3}H]NMS detected the "pirenzepine receptor heterogeneity" in rat brain is an important fact in itself, for the following reasons.

1) There is a large controversy as to whether the receptor heterogeneity detected by pirenzepine reflects the existence of two (or more) different receptor molecules, or of different receptor "states." The demonstration that a classical muscarinic antagonist detected pirenzepine receptor heterogeneity supports the hypothesis that all muscarinic receptors are not equivalent.

2) Most of the studies devoted to the comparison of M1 and M2 receptors draw a parallel between brain (or forebrain) receptors and heart, cerebellum, or ileum receptors. Our results suggest that this approach must be critically evaluated, since the three classes of pirenzepine receptors initially described by Hammer *et al.* (2) are all present in brain areas.

3) The pirenzepine selectivity for A and B sites was low (about 10-fold). The concentration of "M1 receptors" found by [^{3}H]pirenzepine Scatchard plot analysis will therefore be greater than the A receptor concentration, unless tracer binding to B receptors is prevented. Part of the B receptors will also be considered as M1 in all tissues where the three receptor classes are present, when using a nonselective ^{3}H-antagonist in competition studies.

Our results suggested that [^{3}H]pirenzepine dissociated from C but not from B receptors during filtration with ice-cold 50 mM phosphate buffer. This led to significant overestimates of the [^{3}H]pirenzepine K_D value and "M1" receptor concentration, with apparently linear Scatchard plots, using tracer concentration ranges below 50-fold. Saturation curves with a tracer concentration range greater than 100-fold (enclosing both K_D values) are necessary to detect receptor heterogeneity, assuming that the tracer selectivity is close to 10.

It is difficult to demonstrate the existence of different receptor subclasses at equilibrium when the drug selectivity is not very large. However, our results indicate that it is possible to demonstrate receptor heterogeneity in a given preparation, using dissociation kinetics. Furthermore, the affinity of unlabeled drugs for each receptor class can be deduced from competition curves, by allowing the tracer to dissociate from the most rapidly dissociating receptors.

It would be very tempting to associate the receptor classes described in this work with different acetylcholine effects. Indeed, it has been suggested by Raiteri *et al.* (32) that presynaptic autoreceptors (regulating acetylcholine release from hippocampus and cortex), presynaptic heteroreceptors (regulating dopamine release from striatum), and postsynaptic receptors (responsible for the tremorigenic effects of oxotremorine) have different pharmacological specificities. However, it is not yet possible to attempt such a correlation, as far as "second messengers" are concerned. Indeed, the pirenzepine K_i values for adenylate cyclase inhibition and phosphatidylinositol breakdown activation are extremely variable (see Refs. 6–8) and appear to depend on the incubation conditions (6). In view of the very slow antagonist dissociation rates found in this study for the B receptor subclass, equilibration problems might mask the antagonist selectivity and/or the existence of receptor heterogeneity (33). If preincubation with the antagonist is too short, this may indeed lead to an overestimation of the slope of the Schild plot and underestimation of the drugs' affinity (33).

To conclude: (a) dissociation kinetic studies are an excellent test for receptor heterogeneity; (b) three (rather than two) "pirenzepine-binding sites" were present in rat brain; (c) [^{3}H]NMS recognized the "pirenzepine binding-sites" with different kinetic and equilibrium constants; and (d) recognition of the presence of three (rather than two) antagonist-binding sites in rat brain is very important for the correct interpretation of pirenzepine binding, solubilized receptor studies, and physiological studies using selective muscarinic antagonists (including NMS).

[1] Unpublished results.

References

1. Hulme, E. C., N. J. M. Birdsall, A. S. V. Burgen, and P. Mehta. The binding of antagonists to brain muscarinic receptors. *Mol. Pharmacol.* **14**:737–750 (1978).
2. Hammer, R., C. P. Berrie, N. J. M. Birdsall, A. S. V. Burgen, and E. C. Hulme. Pirenzepine distinguishes between different subclasses of muscarinic receptors. *Nature (Lond.)* **283**:90–92 (1980).
3. Venter, J. C. Muscarinic cholinergic receptor structure. Receptor size, membrane orientation and absence of major phylogenetic structural diversity. *J. Biol. Chem.* **258**:4842–4848 (1983).
4. Roeske, W. R., and J. C. Venter. The differential loss of (^{3}H)pirenzepine vs. (^{3}H) (−) quinuclidinylbenzilate binding to soluble rat brain muscarinic receptors indicates that pirenzepine binds to an allosteric state of the muscarinic receptor. *Biochem. Biophys. Res. Commun.* **118**:950–957 (1984).
5. Gilbert, R., S. Rattan, and R. K. Goyal. Pharmacologic identification, activation and antagonism of two muscarine receptor subtypes in the lower esophageal sphincter. *J. Pharmacol. Exp. Ther.* **230**:284–291 (1984).
6. Evans, T., M. M. Smith, L. I. Tanner, and T. K. Harden. Muscarinic cholinergic receptors of two cell lines that regulate cyclic AMP metabolism by different molecular mechanisms. *Mol. Pharmacol.* **26**:395–404 (1984).
7. Brown, J. H., D. Goldstein, and S. B. Masters. The putative M1 muscarinic receptor does not regulate phosphoinositide hydrolysis. Studies with pirenzepine and McN-A343 in chick heart and astrocytoma cells. *Mol. Pharmacol.* **27**:525–531 (1985).
8. Gil, D. W., and B. B. Wolfe. Pirenzepine distinguishes between muscarinic receptor-mediated phosphoinositide breakdown and inhibition of adenylate cyclase. *J. Pharmacol. Exp. Ther.* **232**:608–616 (1985).
9. Vickroy, T. W., H. I. Yamamura, and W. R. Roeske. Differential regulation of high-affinity agonist binding to muscarinic sites in the rat heart, cerebellum, and cerebral cortex. *Biochem. Biophys. Res. Commun.* **116**:284–290 (1983).
10. Vickroy, T. W., W. R. Roeske, and H. I. Yamamura. Pharmacological differences between the high-affinity muscarinic agonist binding states of the rat heart and cerebral cortex labeled with (+)-(^{3}H)cismethyldioxolane. *J. Pharmacol. Exp. Ther.* **229**:747–755 (1984).
11. Flynn, D. D., and L. T. Potter. Different effects of *N*-ethylmaleimide on M1 and M2 muscarinic receptors in rat brain. *Proc. Natl. Acad. Sci. USA* **82**:580–583 (1985).
12. Berrie, C. P., N. J. M. Birdsall, E. C. Hulme, M. Keen, and J. M. Stockton. Solubilization and characterization of high and low affinity pirenzepine binding sites from rat cerebral cortex. *Br. J. Pharmacol.* **85**:697–703 (1985).
13. Lowry, O. H., N. J. Rosebrough, A. L. Farr, and R. J. Randall. Protein measurement with the Folin phenol reagent. *J. Biol Chem.* **193**:265–275 (1951).
14. Scatchard, G. The attraction of proteins for small molecules and ions. *Ann. N. Y. Acad. Sci.* **51**:660–672 (1949).
15. Richardson, A., and A. Humrich. A microcomputer program for the analysis of radioligand binding curves and other dose-response data. *Trends Pharmacol. Sci.* **5**:47–49 (1984).
16. Cheng, Y., and W. H. Prusoff. Relationship between the inhibition constant

(K_i) and the concentration of inhibitor which causes 50 percent inhibition (I_{50}) of an enzymatic reaction. *Biochem. Pharmacol.* **22**:3099–3108 (1973).
17. Potter, L. T., D. D. Flynn, H. E. Hanchett, D. L. Kalinoski, J. Luber-Narod, and D. C. Mash. Independent M1 and M2 receptors: ligands, autoradiography and functions. *Trends Pharmacol. Sci.* 22–31 (1984).
18. Birdsall, N. J. M., E. C. Hulme, and J. M. Stockton. Muscarinic receptor heterogeneity. *Trends Pharmacol. Sci.* 4–8 (1984).
19. Kloog, Y., and M. Sokolovsky. Muscarinic binding to mouse brain receptor sites. *Biochem. Biophys. Res. Commun.* **81**:710–717 (1978).
20. Laduron, P. M., M. Verwimp, and J. E. Leysen. Stereospecific *in vitro* binding of (^{3}H)dexetimide to brain muscarinic receptors. *J. Neurochem.* **32**:421–427 (1979).
21. Gibson, R. E., W. J. Rzeszotarski, E. M. Jagoda, B. E. Francis, R. C. Reba and W. C. Eckelman. (^{125}I) 3-Quinuclidinyl 4-iodobenzilate: a high affinity, high specific activity radioligand for the M1- and M2-acetylcholine receptors. *Life Sci.* **34**:2287–2296 (1984).
22. Kloog, Y., Y. Egozi, and M. Sokolovsky. Characterization of muscarinic acetylcholine receptors from mouse brain: evidence for regional heterogeneity and isomerization. *Mol. Pharmacol.* **15**:545–558 (1979).
23. Gibson, R. E., W. J. Rzeszotarski, W. C. Eckelman, E. M. Jagoda, D. J. Weckstein, and R. C. Reba. Differences in affinities of muscarinic acetylcholine receptor antagonists for brain and heart receptors. *Biochem. Pharmacol.* **32**:1851–1856 (1983).
24. Tien, X. Y., and L. J. Wallace. Trihexyphenidyl—further evidence for muscarinic receptor subclassification. *Biochem. Pharmacol.* **34**:588–590 (1985).
25. Aguilar, J. S., P .J. I. Salas, and E. De Robertis. Cholinergic muscarinic receptor in synaptosomal membranes. Heterogeneity of binding sites for L-[^{3}H]quinuclidinyl benzilate. *Mol. Pharmacol.* **22**:304–309 (1982).
26. Nilverbrant, L. Differentiation of muscarinic receptors. *Acta Physiol. Scand.* **124**(Suppl. 542):106 (1985).
27. Tolkovsky, A. M. Etorphine binds to multiple opiate receptors of the caudate nucleus with equal affinity but different kinetics. *Mol. Pharmacol.* **22**:648–656 (1982).
28. Trifiletti, R. R., M. M. S. Lo, and S. H. Snyder. Kinetic differences between type I and type II benzodiazepine receptors. *Mol. Pharmacol.* **26**:228–240 (1984).
29. Stockton, J. M., N. J. M. Birdsall, A. S. V. Burgen, and E. C. Hulme. Modification of the binding properties of muscarinic receptors by gallamine. *Mol. Pharmacol.* **23**:551–557 (1983).
30. Waelbroeck, M., P. De Neef, P. Robberecht, and J. Christophe. Inhibitory effects of quinidine on rat heart muscarinic receptors. *Life Sci.* **35**:1069–1076 (1984).
31. Gillard, M., M. Waelbroeck, and J. Christophe. *In vitro* effects of gallamine on dissociation kinetics of (^{3}H)*N*-methylscopolamine and (^{3}H)-pirenzepine from rat brain muscarinic receptors. *J. Recept. Res.*, in press.
32. Raiteri, M., R. Leardi, and M. Marchi. Heterogeneity of presynaptic muscarinic receptors regulating neurotransmitter release in the rat brain. *J. Pharmacol. Exp. Ther.* **228**:209–214 (1984).
33. Kenakin, T. P. Effects of equilibration time on the attainment of equilibrium between antagonists and drug receptors. *Eur. J. Pharmacol.* **66**:295–306 (1980).

Send reprint requests to: Dr. Jean Christophe, Department of Biochemistry and Nutrition, Medical School, Université Libre de Bruxelles, Boulevard of Waterloo 115, B-1000 Brussels, Belgium.